SAND2023-08129C

Effects of Hydrogen Isotope Type on Oxidation Rates for Trace Releases

Randy C. Shurtz[a*], Alexander L. Brown[b], Lynelle K. Takahashi[c], Eric N. Coker[d]

[a]Sandia National Laboratories, PO Box 5800, Albuquerque, 87185, USA, albrown@sandia.gov

[b]Sandia National Laboratories, PO Box 5800, Albuquerque, 87185, USA, rshurtz@sandia.gov

[c]Sandia National Laboratories, PO Box 5800, Albuquerque, 87185, USA, lktakah@sandia.gov

[d]Sandia National Laboratories, PO Box 5800, Albuquerque, 87185, USA, encoker@sandia.gov

*Corresponding author

Highlights:

- Tritium fire safety considerations often differ from hydrogen fire safety concerns
- Tritium oxidation kinetics appropriate for simulating fire scenarios are lacking
- Oxidation rate measurements are reported for sub-flammable H_2 and D_2
- Oxidation kinetics for H_2 isotopes are fit to a 1-step model, appropriate for CFD
- A T_2 release is simulated with sub-flammable oxidation in a standard room fire

Abstract:

The fraction of tritium converted to the water form in a fire scenario is one of the metrics of greatest interest for radiological safety assessments. The conversion fraction is one of the prime variables contributing to the hazard assessment. This paper presents measurements of oxidation rates for the non-radioactive hydrogen isotopes (protium and deuterium) at sub-flammable concentrations that are typical of many of the most likely tritium release scenarios. These measurements are fit to a simplified 1-step kinetic rate expression, and the isotopic trends for protium and deuterium are extrapolated to produce a model appropriate for tritium. The effects of the new kinetic models are evaluated via CFD simulations of an ISO-9705 standard room fire that includes a trace release of hydrogen isotope (tritium), illustrating the high importance of the correct (measurement-based) kinetics to the outcome of the simulated conversion.

Keywords: radionuclide fires; tritium hazards; facility safety; operations safety; CFD

1. Introduction

Tritium is a radioisotope of hydrogen (^3H) that produces a low-energy beta particle upon decay and has applications in self-luminous phosphors, fusion energy production, and nuclear weapons. At various U.S. Department of Energy facilities, tritium is stored primarily as a diatomic gas (T_2) or as a solid hydride that can be heated to release T_2 gas. At most of the smaller (i.e., radiological) tritium facilities, the potential flame or explosion hazard is not a major safety

concern since the T_2 inventories are insufficient to sustain a flame, and gases are frequently stored at sub-atmospheric pressures. Nevertheless, T_2 to water conversion in fire environments remains a major safety concern due to radiological hazard considerations; tritiated water vapor is readily absorbed by the human body, making it 10^4 times more hazardous than the same amount of tritium exposure as T_2 gas [1].

Due to the relatively high dose consequence for tritiated water on the human body, the fraction of T_2 that can convert to water vapor is an important factor in tritium safety evaluations. A report reviewing tritium safety [2] has noted that T_2 to T_2O conversions lower than 100% could (in principle) be applied for regulatory safety compliance in specific scenarios with adequate technical support. It is the aim of this work to help provide such technical support. Although extensive literature exists that examines H_2 gas safety involving combustion with high starting pressures and volumes, specific information such as molecular conversion fractions (CFs) and oxidation rates to the water form under low pressures and volumes of typical concern for laboratories with hydrogen inventories are virtually non-existent. Even less information exists for T_2 oxidation rates due to the inherent difficulties of performing experiments that generate radiologically hazardous reaction products from such a rare isotope.

Measured flame speeds for D_2 are slower than measured for H_2 [3-5], consistent with early observations of slower reaction rates for heavier isotopes [6]. In principle, these measurements could be used to estimate even slower flames speeds for T_2 that would be applicable to releases above the lower flammability limit (LFL). However, T_2 containers in many facilities operate at low or even sub-atmospheric pressures; leaks from these are likely to result in concentrations mostly below the LFL, which is the regime of focus for this paper. Flammable concentrations arising from tritium stored at sub-atmospheric pressures is not a likely scenario [7].

To our knowledge, no prior literature considers high-temperature oxidation rates of hydrogen isotopes in this low-concentration regime (where the non-radioactive isotopologues pose minimal safety hazard), especially in terms of simplified global kinetics suitable for large-scale simulations. There are a few studies of initial elementary steps in the oxidation process for H_2 and D_2 [8-11], but it is not clear whether these are sufficiently comprehensive to derive global oxidations rates for distinct hydrogen isotopes that are applicable at very low concentrations.

Several studies measured kinetic rate constants for oxidation of tritium in air at room temperature over timescales of many days, including a wide range of concentrations [12-16]. However, these results do not include temperature dependence (i.e., activation energies) that would be needed to extrapolate such rates to temperatures of several hundred degrees Celsius over timescales of seconds or possibly much shorter. Additionally, the very short oxidation timeframes in fires are likely too fast for oxidation rates of dilute mixtures to be significantly catalyzed by beta decay, whereas such an effect was observed by these investigators over much longer timescales.

To address these critical knowledge gaps, this paper reports measurements of the non-radioactive isotopologues of diatomic hydrogen (H_2, D_2) in air at low concentrations (sub-flammable) over a range of temperature and flow conditions in a tube reactor. The principal metric measured and reported is the extent of conversion to water. The experimental data from the tube reactor experiments are used to gauge isotopic trends for hydrogen oxidation rates, which are interpreted via computational fluid dynamics (CFD). These trends are then extrapolated to produce kinetic rate parameters appropriate for tritium oxidation at low concentrations of relevance to radiological tritium facilities. Finally, the impact of the derived kinetic rate parameters on

conversion of a hydrogen isotope at low concentration in a room-scale fire scenario is demonstrated through CFD simulations.

2. Experimental Methods

Hydrogen isotope oxidation tests were carried out within a quartz glass cylindrical tube (internal diameter 13.5 mm, length 420 mm) in a tube furnace under a range of H_2 (D_2): air ratios, gas flow rates, and temperatures. The hydrogen inlet was 2.5 cm inside the quartz glass tube, whereas the air flow entered the system further upstream. The hydrogen inlet tube was a piece of stainless-steel tubing (outer diameter 3.175 mm, inner diameter 1.75 mm) centered within the quartz. The gas within the quartz tube was maintained at atmospheric pressure, which in Albuquerque, NM is typically 635 Torr. Hydrogen gas (99.999%), deuterium gas (99.999%) and synthetic air (ultra-zero grade) were acquired from Matheson TriGas and used without further purification. Mass flow controllers were used for gas flows (MFCs, Brooks). The MFCs were calibrated using a bubble-meter, and flows are reported at standard temperature and pressure. The gas composition was monitored downstream of the quartz tube using a gas chromatograph (GC, Agilent 3000A). A cold finger was installed downstream of the quartz tube to condense out most of the water product and thereby prevent flooding of the GC separation column.

Once stable gas flows were achieved (as determined by GC output, typically within 10-15 mins of initiating gas flow) and the GC had been calibrated, the tube furnace was heated rapidly (stepwise) to 500°C and allowed to stabilize. No hydrogen isotope oxidation was observed at 500°C under any of the conditions used in this study, and this was used as the calibration point for the GC. The downstream cold finger was immersed in ice, and the furnace was programmed to heat at a rate of 1°C/min from 500°C to either 750°C or 800°C, hold for 15 minutes, and then cool at 1°C/min to 500°C. The GC drew a sample of the gas exiting the quartz tube approximately every three minutes throughout the entire experiment, and outlet conversion was calculated from the H_2 or D_2 concentration with respect to the calibration condition at 500°C [7].

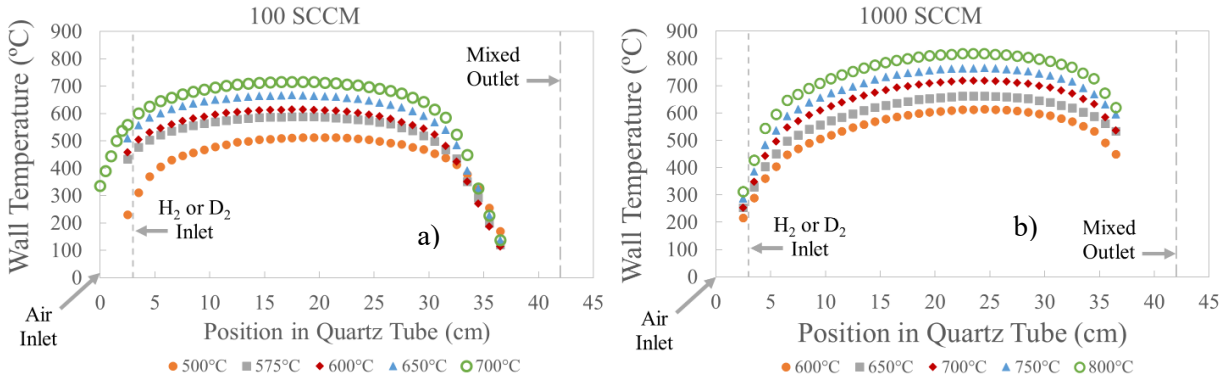

Fig. 1. Temperature profile measurements used as boundary conditions for the quartz wall.

Fig. 1 presents steady-state temperature measured along the interior wall of the quartz tube. This was done by inserting a 1/8" diameter K-type thermocouple probe through the outlet with only air flowing. Hydrogen concentrations in the oxidation experiments were low enough to neglect thermal effects of hydrogen oxidation for the boundary conditions (BCs). Temperatures near the ends of the tube were less accessible using this approach but were sufficiently low (<< 500°C) to

be considered non-critical for modeling reaction rates. The furnace control temperatures used to designate thermal conditions in this paper are designated in the legends and are all near the plateaus in Fig. 1. Conditions with higher inlet airflow are expected to cool the inlet upstream of the heat source more efficiently, so the lower measured wall temperatures near the H_2 inlet shown in Fig. 1b at 1000 standard cubic centimeters per minute (SCCM) with respect Fig. 1a at 100 SCCM are reasonable.

3. Computational Methods

SIERRA/Fuego [17, 18] is a low-Mach number code for simulating objects in fires and is extended to support a variety of problems of interest to Sandia and affiliates who use the code. A major differentiating factor is that the code is a control volume finite element mechanics (CVFEM) code rather than a more traditional control volume code. A variety of mesh elements are available to the unstructured solver. The mesh for the fire simulations in this study is hexahedral and regular, which would be suited to a structured code solver as well. Tetrahedral elements were employed for 3-dimensional (3-D) simulations and triangular elements of with comparable length scales were used for 2-D simulations; this choice facilitated meshing features of different sizes present in the experimental geometry. Fuego is massively parallel, and the resolved scale for these simulations is in the 0.1-100 cm range.

A variety of turbulence and reaction models exist, with this work electing to represent turbulence effects using the Temporally Filtered Navier-Stokes (TFNS) model (a hybrid LES/RANS capability) [19]. A fire in the corner of the simulated ISO-9705 standard room [20] was represented using the Eddy Dissipation Concept (EDC) model for fluid (gas)-phase reactions [21, 22]. The EDC model permits a single fuel. This effort simulates the fire with a methane gas release. Due to this limitation, the reaction of tritium to oxide is solved separately through a 1-step mechanism that is external to the EDC model, with separate tritium species variables.

Participating media radiation energy transport is simulated using Nalu coupling [17], which mostly involves a heat loss from the fire to the surroundings. Nalu uses a Discrete Ordinates solver to solve the radiative transfer equation. Participating species include soot, CO_2, and H_2O using a gray approximation. The radiation contribution of released vapors is neglected and believed to be small due to the low concentrations. The walls and ceiling are simulated with a 1D conduction model and thermal properties consistent with the ISO standard (600 kg/m^3 density, 20 mm thick). Walls become heated over the duration of the burn, providing thermal feedback.

All cases were run with version 4.56.4 of the SIERRA/Fuego code. Designed under the governance of DOE order O 414.1D, version control, nightly testing, and verification are inherent in the code design and maintenance practices that lend to the credibility of the results. Validation involves benchmarking the solutions to datasets, which help establish the accuracy of the modeling. A campaign to validate the code resulted in numerous component validation results beginning approximately 20 years ago. More recent and relevant validation efforts include a comparison to a dispersion in an urban geometry [23], and a comparison to a buoyant plume of He gas [7, 24].

3.1 Simulated Tube Reactor

The simple geometry of the tube reactor closely approximates a 1-D plug flow reactor (PFR), so the hydrogen oxidation is dominated by the temperature profile and the residence time. Turbulence (which is expected at Reynolds numbers between 10,000 and 440,000 calculated for the tube reactor) improves the PFR approximation and hence the kinetic rate measurements by ensuring radially uniform heating of the gas mixture and efficient mixing of H_2 or D_2 with air before the flowing gas achieves temperatures high enough for oxidation to occur. The main reasons for pursuing a CFD simulation for these kinetic studies rather than a simpler 1-D PFR simulation were (1) to obtain a pre-test indication of whether good mixing could be expected before the hydrogen encountered high temperatures and (2) to prepare for the simulations described in Section 3.3 by implementing the kinetics in a comparable but simplified SIERRA/Fuego simulation scenario.

A 3-D mesh was used for pre-test simulations to verify that mixing was essentially complete by the time the centerline gas temperature reached 325°C [7]. This is well below temperatures where conversion to water was first observed (> 500°C). Simulations comparing 3-D meshes and 2-D axisymmetric meshes are reported separately [7]. It was found that differences in final conversion and steady-state profiles of centerline temperature, velocity, and concentrations were minimal between 3-D and 2-D meshes with identical mesh size parameters, while the computational expense was reduced by a factor of 40 for the 2-D mesh. Results were also consistent for 3 levels of mesh refinement in 2-D and 3-D; the worst-case deviation was 4% of nominal conversion, or 2.5% deviation in absolute conversion units [7].

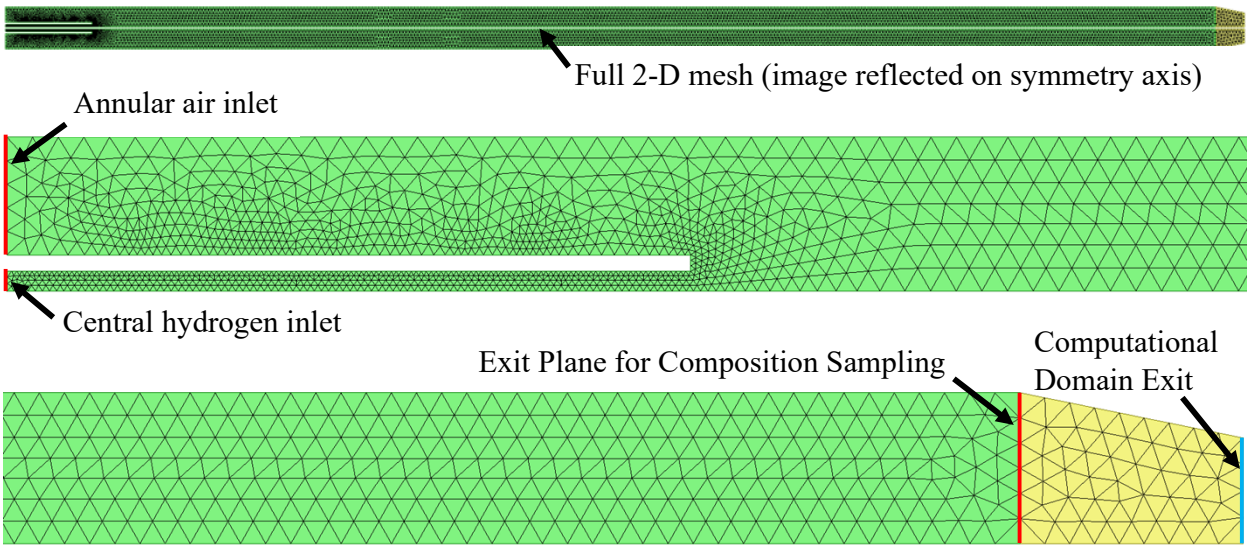

Fig. 2. Mesh used to model the H_2 and D_2 oxidation experiments, including zoomed views of the inlet and outlet (artificial contraction in yellow is for computational stability).

The top view in Fig. 2 includes normal and mirrored perspectives of the 2-D axisymmetric mesh used for most of the simulations shown in Section 4.1 to illustrate the entire domain with the axis of symmetry. The magnified view of the inlet in the middle panel of Fig. 2 has two vertical red edges of different sizes on the far left, representing BCs for the annular air inlet and the central hydrogen inlet tube. Both inlet BCs are specified in terms of velocity vectors, temperature (300

K or 27°C) and composition. The yellow contraction in Fig. 2 is an artificial extension that was appended to the green representation of the experimental geometry. This yellow conical region was designed to ensures that outlet concentrations at the designated sampling plane (red, at the axial position of the experimental exit plane) were not influenced by spurious backflow (not observed with this geometry) from the simulated domain outlet (defined as air at 300 K or 27°C). The simulated domain outlet (blue line) was defined as an open or outflow boundary condition.

3.2 Hydrogen Isotope Properties and Reaction Modeling in SIERRA/Fuego

Hydrogen and deuterium properties are available in standard references, but very few measurements are available for tritium. Thermophysical properties for isotopologues of hydrogen and water that were recently identified [7], along with methods used to deduce properties for tritium species that could not be found in literature. These temperature-dependent properties were used to simulate hydrogen isotopes in this study.

SIERRA/Fuego includes a capability to model user-defined reactions [17]. Hence, Fuego simulations with the geometry in Fig. 2 accounted for flow, mixing, heating, reaction (water formation) and cooling. The modeling parameters for kinetic rates were iteratively optimized using the CFD code. A global hydrogen oxidation mechanism from Marinov et al. (1995) [25] was initially selected for this work:

$$r_{global} = Aexp\left(-\frac{E}{RT}\right)[H_2]^{n_H}[O_2]^{n_O} \quad (1)$$

The default reaction orders of $n_H = 1.0$ and $n_O = 0.5$ specified in this equation are consistent with the stoichiometry of the global oxidation reaction ($H_2 + ½\ O_2 \rightarrow H_2O$). We have adapted the originally reported rate constants for this reaction to units required by Fuego with concentrations in mol/m^3 (indicated by square brackets). The originally reported Arrhenius parameters were calibrated to flame speed data [25], but the regime of interest for this work corresponds to sub-flammable hydrogen concentrations (far below 4% in air at atmospheric pressure) [26, 27]. Other H_2 kinetic models exist, and were also considered, including for example [28-38].

Arrhenius rate constants are defined as $k = Aexp(-E/RT)$, as in Equation (1). A relationship for isotopic pairs of Arrhenius rate constants may be derived from kinetic (collision) theory of gases, where molecular velocities are inversely related to the square root of molecular weight. This relationship is given by [39, 40]:

$$\left(\frac{k_H}{k_T}\right) = \left(\frac{k_H}{k_D}\right)^{1.44} \quad (2)$$

where the subscripts H, D and T refer to normal hydrogen (protium), deuterium, and tritium. The exponent of 1.44 is defined using the following function of atomic masses [39, 40]:

$$\frac{1-\sqrt{\frac{m_H}{m_T}}}{1-\sqrt{\frac{m_H}{m_D}}} = 1.44 \quad (3)$$

Equation (2) neglects quantum effects such as tunneling, which may become non-negligible at the high temperatures investigated in this work. However, Equation (2) has been successful in describing experimental trends over a very broad range of conditions [39, 41, 42] and is expected to capture the most important aspects of the isotopic trend in reaction rates. Equation (2) is recommended as the best available method to scale the experimentally derived pre-exponential factors from protium and deuterium to produce the recommended value for the tritium rate constant. A common activation energy yielded an acceptable fit of the experimental oxidation measurements for H_2 and D_2, so the same activation energy was assumed for T_2 with a pre-exponential factor calculated from Equation (2).

Equation (1) was selected as a sufficiently simple chemical rate expression for application in the CFD simulations of the ISO-9705 scenario [20] described in Section 3.3. It is normally not advisable to simulate fire scenarios with direct kinetic mechanisms such as this because flames are typically ~1 mm in scale and the resolution required to resolve this is not generally available for fire problems of practical interest. Besides the resolution problem, stiff reactions can also be challenging to solve with accuracy. The EDC model is designed to produce approximations to fires in under-resolved scenarios and is a mixing-limited approximation. The use of the global 1-step mechanism is thought to be reasonable for the hydrogen contaminant reactions in this circumstance because:

1. The hydrogen oxidation reactions are not expected to occur under flaming environments with the low-concentration leaked hydrogen as the primary fuel source.
2. The reactions are very non-linear with temperature, and cell average temperatures in the vicinity of the EDC-heated plume (with a steady, uniform source of flow) are probably adequate to capture the bulk extent of reaction for the hydrogen isotopes.
3. There is a degree to which the reactions will be advection and/or diffusion controlled, this being the case the mechanism can be approximate and may still yield acceptable results.

Because the fire in the ISO-9705 simulations is intended only as a heat source, simulating it with the EDC model is an acceptable approximation for a fire condition as it affects the reaction of the contaminant release of hydrogen. The EDC fuel is CH_4, and the inflow is selected to give a heat release rate for the reaction as specified in the ISO-9705 standard [20] and Section 3.3 below.

3.3 Simulated ISO9705 Standard Room Fire with Hydrogen Isotope Release

It was not obvious in advance whether the oxidation rates developed in this work for low concentrations would have an important influence on the extent of hydrogen isotope oxidation in a reasonable room-scale fire scenario. The ISO-9705 (2016) standard [20] was selected as a representative fire scenario to evaluate via simulation in conjunction with a release of hydrogen isotope contaminant. This standard prescribes a 3.6-m by 2.4-m room 2.4 m high with a doorway of 2.0 m height and 0.8 m width centered along one of the 2.4 m walls, as shown in Fig. 3. A 170-mm square gas burner surface is prescribed, and this dimension is used to locate a methane injection on the ground in the corner furthest from the doorway of the domain. The contaminant is released from a similarly dimensioned boundary condition in the other corner with comparable distance from the door. The standard fire is prescribed as 100 kW, with the potential for

increasing the output to 300 kW at 10 minutes and continuing the test for an additional 10 minutes. The simulations in this work modified these guidelines by specifying the larger 300 kW fire throughout to ensure that conversions of T_2 to T_2O from a small release would be high enough for useful comparisons. The release of hydrogen isotope is not part of the standard, so the release was assumed to be 0.1 g occurring between 10 s and 16.5 s at a constant rate.

To model the fire, an extended flow region outside the doorway is added to allow for natural ventilation conditions that would be more representative of the ISO-9705 tests. An open boundary is applied to the periphery of this extension of the domain. During tests, the open door provides an escape path for hot products towards the top, and an inflow of fresh air towards the bottom naturally develops under these conditions, which helps sustain the fire. This causes a net movement of tritium and hot gases upward due to buoyancy and towards the domain exit through the door, which is from lower left to upper right on the central results plane designated in Fig. 3. The ISO-9705 mesh used for this study has a mesh length scale of 4.25 cm, which is double the length-scale refinement of 8.5 cm shown in Fig. 3 (about a factor of 8 increase in mesh elements). This mesh length of 4.25 cm was found to produce results in a convergence study that were adequately similar to simulations with an even more refined mesh length scale of 2.83 cm (triple the length-scale refinement shown in Fig. 3, or a factor of about 27 increase in mesh elements). These results are presented in more detail in a separate technical report [7].

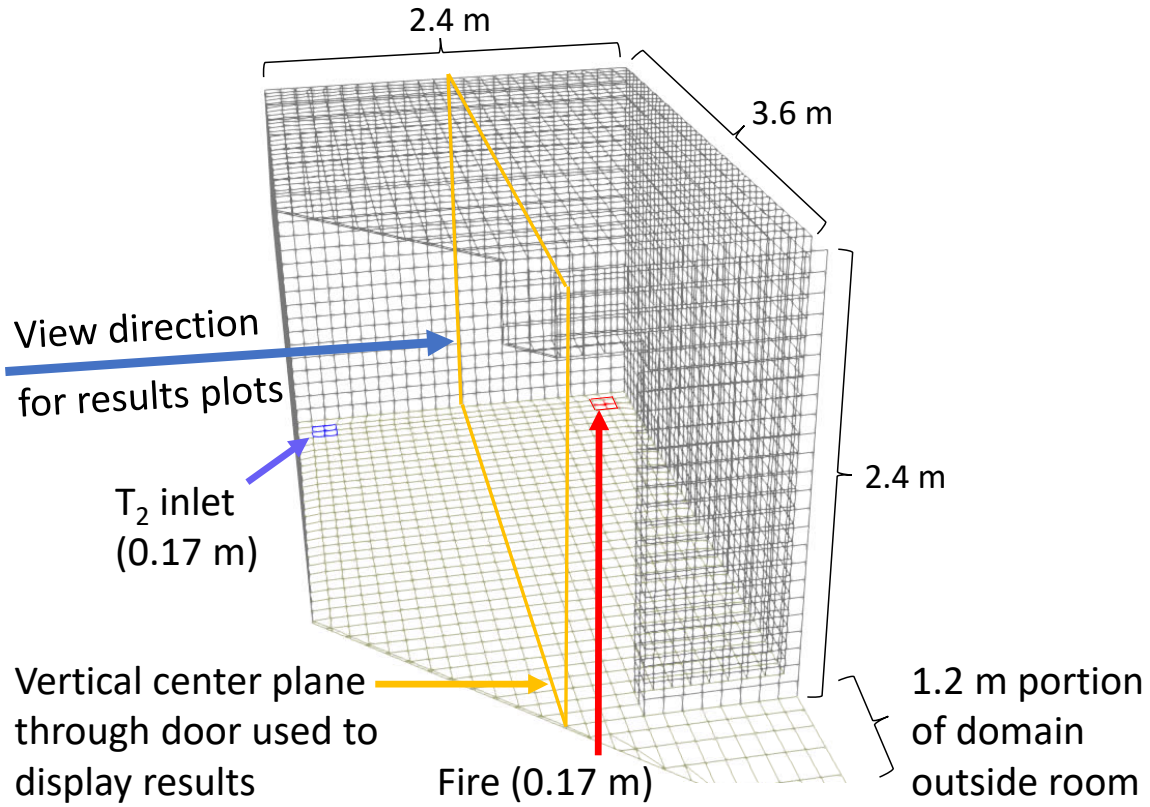

Fig. 3. Geometry used to model the ISO-9705 room fire scenario with corner removed for visibility and results plane outlined in gold. The mesh used has twice the refinement shown.

The ISO-9705 standard room is conservatively small with respect to industrial and laboratory spaces where tritium is typically stored. The tritium concentrations that can exist within it are therefore maximized. A second conservatism is the lack of any ceiling ducts within the room; active ventilation is nearly universal and even ducts with no airflow can provide an escape path for either hot gases or hydrogen isotopes that rise to the ceiling.

4. Results and Discussion

4.1 Oxidation Measurements and Kinetic Modeling

For brevity, the oxidation data for H_2 and D_2 are presented in terms of conversion versus temperature in combination with the optimized simulations at a subset of temperatures. The original kinetic parameters [25] for Equation (1) caused simulated oxidation of hydrogen to occur at temperatures about 250°C lower than the measurements [7]. Therefore, several parameter adjustments were required to represent the measurements. Equation (1) is a global mechanism that omits details inherent in the underlying elementary reaction steps; it cannot predict all conversion profiles features over the full range of possible experimental conditions.

The finalized parameters for Equation (1) are listed below the original values [25] in Table 1; the rate parameters are numbered in the leftmost column as R1 through R4 for convenience. Manual parameter adjustment to produce a good visual fit of the data was most efficient when the activation energy E was adjusted first, followed by the hydrogen reaction order n_H. The pre-exponential factor A was updated for each intermediate step to ensure a good match of the target data. The default oxygen reaction order of $n_O = 0.5$ was retained because measurements with varying oxygen were lacking; this is adequate when oxygen concentration does not vary much.

Table 1. Kinetic parameters for oxidation of trace concentrations of hydrogen isotopes using Equation (1). The tritium pre-exponential factor is extrapolated via Equation (2).

#	Isotope and Source	Molecular Mass (g/mol)	A	E/R (K)	n_H
R1	H_2 (protium, [25])	2.016	$1.77\text{x}10^{10}$ $m^{1.5}/mol^{0.5}/s$	17,600	1.0
R2	H_2 (protium, this work)	2.016	8.0×10^{24} $m^{4.5}/mol^{1.5}/s$	50,000	2.0
R3	D_2 (deuterium, this work)	4.028	4.0×10^{24} $m^{4.5}/mol^{1.5}/s$	50,000	2.0
R4	T_2 (tritium, extrapolated)	6.032	2.9×10^{24} $m^{4.5}/mol^{1.5}/s$	50,000	2.0

Fig. 4 highlights a subset of conditions with H_2 or D_2 concentrations of 0.1% used to determine activation energy. Symbols without lines are measurements, and open symbols with lines are optimized simulations with rates from Table 1 (R2 for H_2, R3 for D_2). Differences in residence time from 2 magnitudes of airflow are the principal cause of the horizontal shift between about 600°C and 650°C. The magnitude of this horizontal shift and the slope of the conversion curves both increase with the activation energy E. It was apparent from the low slopes of the initial simulated conversion curves that activation energies much larger than the published value of E/R =

17,600 K [25] (derived from measurements in the flammable regime) would be required. The revised activation energy (E/R = 50,000 K) with the pre-exponential factors in Table 1 yield simulated conversions that agree with measured onset behavior, which is defined here as conversions between 5% and 20%. For simplicity, the same activation energy was used for H_2 and D_2. Some literature suggests higher activation energies may apply to heavier isotopologues [39], but this approach was rejected because doing so would produce a worse fit of our measurements.

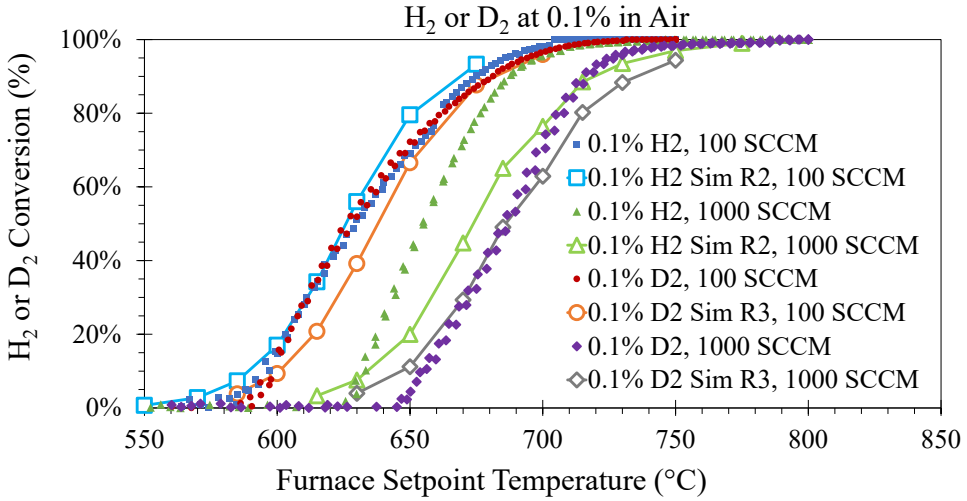

Fig. 4. Experimental and simulated conversion of H_2 and D_2 at 0.1% in air; rates from Table 1

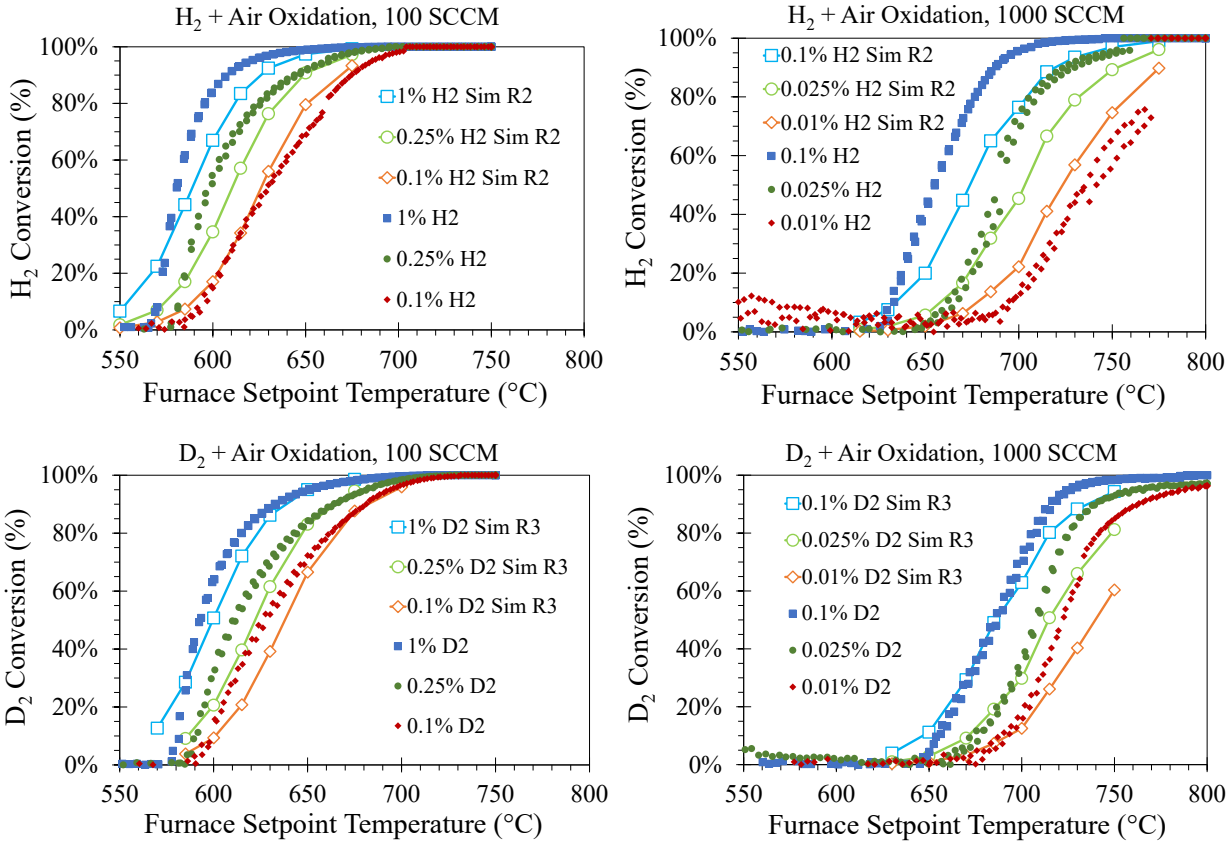

Fig. 5. Experimental and simulated conversion of H_2 (top, R2) and D_2 (bottom, R3) with long residence time (left, 100 SCCM airflow) and short residence time (right, 1000 SCCM airflow).

Fig. 5 shows that the full set of oxidation measurements are of good quality. Minor hysteresis occurs only at the lowest flow rates for H_2 or D_2 (see far right series). The optimized simulations compare favorably to these data. Attempts to model oxidation with the default hydrogen reaction order of $n_H = 1.0$ would produce identical results for all simulations (open symbols) shown within each panel of Fig. 5. This makes sense for a first-order reaction with an identical temperature history because the higher average reaction rates are proportional to the higher initial reactant concentration, and these factors cancel out when the data are normalized as fractional conversions. Parameter scoping exercises indicate that values of n_H closer to 3.0 yield too much vertical separation between conversion curves for both D_2 and H_2. An integer value for n_H is preferred given the experimental uncertainty and because the units for the pre-exponential factor are greatly simplified. The optimal reaction order of $n_H = 2.0$ from Table 1 yields the best vertical separation between different inlet concentrations in Fig. 5 at temperatures where the lowest concentrations (open orange diamonds) have conversions of 10% or lower.

Although oxidation rates for deuterium and protium had measurable differences for some experimental conditions, these measured rates and the extrapolated tritium oxidation rates from Table 1 are all of the same order of magnitude. The rate reduction in the sub-flammable regime (R2 through R4 in Table 1) compared to rates for flammable concentrations (R1 in Table 1) is a much more pronounced effect, increasing onset temperatures by about 250°C. The uncertainties associated with the kinetic fits to Equation 1 and the extrapolation via Equation 2 are not well established at this writing, but it is apparent that these uncertainties are orders of magnitude lower than errors resulting from applying flammable kinetic rates to the sub-flammable regime.

4.2 Effect of Kinetic Models on Tritium Oxidation with a Simulated ISO-9705 Fire

Selected results from two SIERRA/Fuego CFD simulations of a tritium release in the ISO-9705 room shown in Fig. 3 were used to investigate effects of the updated hydrogen isotope oxidation kinetics in a full-scale 300-kW fire scenario. Fig. 6 shows T_2 and T_2O concentrations in the center-plane of the simulated room with oxidation rates based on flaming H_2 (R1 from Table 1) and sub-flammable T_2 (R4 from Table 1, as developed in this work). The results plane through the center of the door at 67 seconds was chosen to illustrate maximum T_2O and the dispersion path through the door.

Hot gases from the fire rise to the ceiling, and any T_2 migrating into regions with sufficiently high temperatures can react to form T_2O (approximately 550°C to 800°C, as shown in Fig. 5). "Flammable" T_2 above a conservatively low LFL of 4% from H_2 (Cadwallader et al. estimated the T_2 LFL as 6.6% [43]) is localized to the time and (cold) vicinity of the T_2 release event with a maximum volume of 792 cm^3. This is equivalent to a 2.74-cm thick layer above the injection plane. The maximum scale for T_2 shown in Fig. 6 corresponds to 1% of this conservative LFL.

The T_2 concentrations shown as light blue in Fig. 6 are equivalent to the lowest inlet concentrations measured in the tube furnace for H_2 and D_2, so the highest simulated reaction rates appear to be within the range of the measurements used to derive the sub-flammable kinetics. The maximum scale for T_2O shown in Fig. 6 corresponds to 0.25% of what would be

expected before dispersion of a mixture at the 4% LFL when fully oxidized. The T_2O concentration is near its maximum at 67 s, which is why this time was chosen for the images in Fig. 6 (nearly 1 minute after the release ends).

The thin regions enriched in unconverted T_2 escaping through the doorframe just below the hot gas layer shown on the left panels of Fig. 6 are nearly identical. As expected, the maximum T_2 concentration is higher with the updated (slower) oxidation rates because less is consumed. T_2 concentrations are maximized just below the hot layer of gas due to diffusive and advective transport from the release, flow behaviors induced by the fire, and consumption in the hot zone. The region with T_2O in the hot layer near the ceiling is much larger with the faster oxidation rates originally derived from flaming H_2 [25], with an overall T_2 oxidation CF of 15.43% for the full simulated duration (180 s). The slower rates derived in this study (more appropriate for the concentration regime of these simulations) produce only a small region of T_2O with lower maximum concentrations and an overall CF of 4.72% with respect to the released T_2.

Thus, updating the kinetics reduced conversion of T_2 to T_2O by a factor of 3.27 at the conditions simulated. Conversion in both versions of this scenario is limited by the extent that T_2 mixes with hot gas, and it could easily be assumed that the effect of chemical kinetics would not strongly affect a scenario where mixing dominates. The large difference in conversion with different oxidation rate models is attributable to the fact that the volume of gases that exceed the higher temperature threshold of about 550°C associated with the sub-flammable kinetics is small compared to the volume of gases that exceed the lower threshold of about 300°C associated with the flaming kinetic rates. Hence, little or no conversion occurs for T_2 that encounters maximum temperatures between 300°C and 550°C when the kinetics developed in this work are used, whereas significant conversion of T_2 occurs in this temperature range if oxidation rates based on flaming kinetics are assumed. It was not obvious before this study that the oxidation rates at low concentrations would be so much slower than rates derived from the flaming regime, which made the effect of kinetics significant even in this room-scale fire scenario.

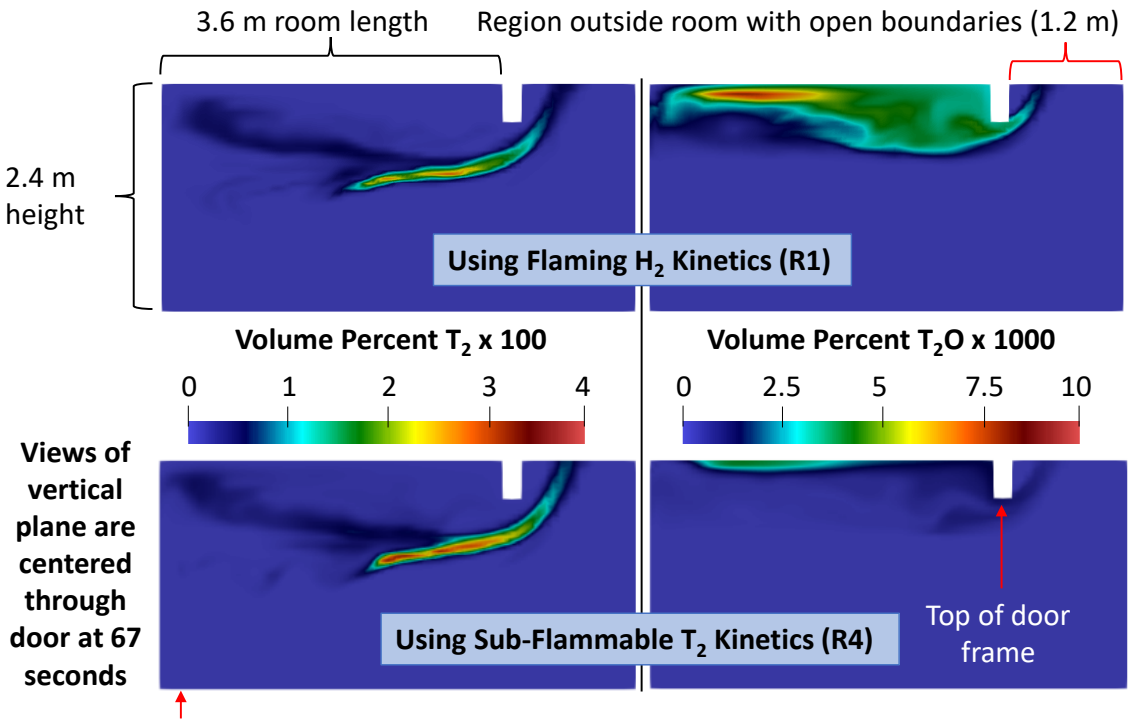

Fig. 6. Simulated volume fractions of T_2 (left views) and T_2O (right views) in ISO-9705 room (plane shown in Fig. 3) using different oxidation rates from Table 1.

5. Summary and Conclusions

This work reports oxidation measurements for H_2 and D_2 at sub-flammable concentrations in a tube furnace, with five concentrations from 0.01% to 1% by volume in air. Oxidation to the water form (H_2O or D_2O, respectively) occurred between 550°C and 800°C, and the rates of protium conversion exceeded the deuterium oxidation rates for most experimental conditions. These experimental trends suggest that tritium should have oxidation rates lower than the measured deuterium rates reported in this study, but on the same order of magnitude. Furthermore, the hydrogen oxidation rates reported in this work were significantly slower than predicted by a global 1-step reaction model that was originally developed from high-concentration measurements in the flammable regime [25]; the measured threshold for the onset of H_2 oxidation increased by about 250°C with respect to pre-test simulations with the rate expression derived for flaming reactions.

Rate parameters for the global 1-step hydrogen oxidation reaction [25] were adapted in this work to model the experimentally measured conversions, using a common apparent reaction order and activation energy for H_2 and D_2 in the low-concentration regime. The final activation energy obtained for this regime was much higher than reported for the flammable regime, which is consistent with the low measured rates. The same reaction order and activation energy are recommended for T_2 oxidation, while the tritium pre-exponential factor was extrapolated to a lower value based on the experimental trends observed for protium and deuterium oxidation.

These results have safety implications for tritium, as the hazard level for a release scenario is largely determined by the fraction of released tritium that is converted to the more hazardous water form (T_2O or THO). The low measured oxidation rates for H_2 and D_2 and the expected reduction in oxidation rates for T_2 with respect to the lighter hydrogen isotopes both imply that a substantial fraction of tritium released in a credible low-concentration scenario could remain unoxidized in the vicinity of a heat source such as a fire. The global rate expression with the parameters recommended in this study are intended to facilitate comparisons to other data sources and to provide an alternative means to evaluate the hazards of tritium release scenarios with respect to the non-informed initial regulatory assumption of 100% oxidation [1].

CFD simulations employing an ISO-9705 standard fire geometry and fire with an adjacent release of T_2 demonstrate that limited oxidation can be expected in a representative room fire scenario with a release of hydrogen isotope contaminant. The conversion fraction to T_2O is greatly reduced by the slower oxidation rates derived from our measurements in a low-concentration regime. This is attributable to the much smaller volume of hot gas above the higher oxidation threshold associated with the slower rates developed in this work. These simulated results are valuable because it was not clear *a priori* that the reduced oxidation rates at low concentrations would be substantial enough to cause a strong interaction between mixing and kinetic effects.

Acknowledgements

This article has been authored by an employee of National Technology & Engineering Solutions of Sandia, LLC under Contract No. DE-NA0003525 with the U.S. Department of Energy (DOE). The employee owns all right, title and interest in and to the article and is solely responsible for its contents. The United States Government retains and the publisher, by accepting the article for publication, acknowledges that the United States Government retains a non-exclusive, paid-up, irrevocable, world-wide license to publish or reproduce the published form of this article or allow others to do so, for United States Government purposes. The DOE will provide public access to these results of federally sponsored research in accordance with the DOE Public Access Plan https://www.energy.gov/downloads/doe-public-access-plan.

References

[1] *Tritium Handling and Safe Storage*, DOE-STD-1129-2015, Washington, D.C., (2015).

[2] J. Mishima and C. M. Steele, *Oxidation of Tritium Gas Under Accident and Transport Conditions*, LA-UR-02-3803, (July 2002).

[3] P. Gray, S. Holland, and D. B. Smith, "The effect of isotopic substitution on the flame speeds of hydrogen-oxygen and hydrogen-nitrous oxide flames," *Combustion and Flame,* vol. 14, no. 3, pp. 361-374, (1970), doi: https://doi.org/10.1016/S0010-2180(70)80050-5.

[4] P. Gray and D. B. Smith, "Isotope effects on flame speeds for hydrogen and deuterium," *Chemical Communications (London),* 10.1039/C19670000146 no. 4, pp. 146-148, (1967), doi: https://doi.org/10.1039/C19670000146.

[5] G. W. Koroll and R. K. Kumar, "Isotope effects on the combustion properties of deuterium and hydrogen," *Combustion and Flame,* vol. 84, no. 1, pp. 154-159, (1991), doi: https://doi.org/10.1016/0010-2180(91)90044-C.

[6] C. N. Hinshelwood, A. T. Williamson, and J. H. Wolfenden, "The Reaction Between Oxygen and the Heavier Isotope of Hydrogen," *Proceedings of the Royal Society of London. Series A, Mathematical and Physical Sciences,* vol. 147, no. 860, pp. 48-57, (1934). [Online]. Available: http://www.jstor.org/stable/2935460.

[7] A. L. Brown, R. C. Shurtz, L. K. Takahashi, E. N. Coker, J. C. Hewson, and M. L. Hobbs, *Tritium Fires: Simulation and Safety Assessment*, Sandia National Laboratories, SAND2022-4187, (April 2022). Available: https://doi.org/10.2172/1862102

[8] A. A. Westenberg and N. de Haas, "Atom—Molecule Kinetics Using ESR Detection. III. Results for O+D2→OD+D and Theoretical Comparison with O+H2→OH+H," *The Journal of Chemical Physics,* vol. 47, no. 10, pp. 4241-4246, (1967), doi: https://doi.org/10.1063/1.1701606.

[9] K. M. Pamidimukkala and G. B. Skinner, "Resonance absorption measurements of atom concentrations in reacting gas mixtures. VIII. Rate constants for O+H2→OH+H and O+D2→OD+D from measurements of O atoms in oxidation of H2 and D2 by N2O," *The Journal of Chemical Physics,* vol. 76, no. 1, pp. 311-315, (1982), doi: https://doi.org/10.1063/1.442779.

[10] J. V. Michael, "Rate constants for the reaction O+D2→OD+D by the flash photolysis–shock tube technique over the temperature range 825–2487 K: The H2 to D2 isotope effect," *The Journal of Chemical Physics,* vol. 90, no. 1, pp. 189-198, (1989), doi: https://doi.org/10.1063/1.456513.

[11] P. Marshall and A. Fontijn, "HTP kinetics studies of the reactions of O(2 3PJ) atoms with H2 and D2 over wide temperature ranges," *The Journal of Chemical Physics,* vol. 87, no. 12, pp. 6988-6994, (1987), doi: https://doi.org/10.1063/1.453395.

[12] L. M. Dorfman and B. A. Hemmer, "Ion-Pair Yield of the Tritium-Oxygen Reaction," *The Journal of Chemical Physics,* vol. 22, no. 9, pp. 1555-1558, (1954), doi: https://doi.org/10.1063/1.1740456.

[13] J. E. Phillips and C. E. Easterly, *Tritium oxidation and exchange: preliminary studies*, Oak Ridge National Laboratory, United States, ORNL/TM-5963, (May 1, 1978). Available: https://doi.org/10.2172/7157724

[14] P. J. Papagiannakopoulos and C. E. Easterly, "Mechanism of HTO Formation in Gaseous Tritium Mixtures," *International Journal of Chemical Kinetics,* vol. 14, pp. 77-90, (1982). [Online]. Available: https://doi.org/10.1002/kin.550140109.

[15] C. E. Easterly and M. R. Bennett, "Radiation Catalyzed Conversion of Tritium Gas to Tritiated Water," *Nuclear Technology - Fusion,* vol. 4, no. 2P2, pp. 116-120, (1983), doi: https://doi.org/10.13182/FST83-A22854.

[16] C. E. Easterly, H. Noguchi, and M. R. Bennett, "Low Concentration Conversion of Tritium Gas to Tritiated Water," *Fusion Technology,* vol. 8, no. 2P2, pp. 2564-2568, (1985), doi: https://doi.org/10.13182/FST85-A24665.

[17] SIERRA Thermal/Fluid Development Team, *SIERRA Low Mach Module: Fuego User Manual - Version 4.58*, Sandia National Laboratories, SAND2020-11536, (October 2020). Available: https://doi.org/10.2172/1716571

[18] SIERRA Thermal/Fluid Development Team, *SIERRA Low Mach Module: Fuego Theory Manual - Version 4.58*, Sandia National Laboratories, SAND2020-11535, (October 2020). Available: https://doi.org/10.2172/1716570

[19] S. R. Tieszen, S. P. Domino, and A. R. Black, *Validation of a simple turbulence model suitable for closure of temporally-filtered Navier-Stokes equations using a helium plume*,

Sandia National Laboratories, SAND2005-3210, (June 2005). Available: https://doi.org/10.2172/923079

[20] *Reaction to fire tests - Room corner test for wall and ceiling lining products - Part 1: Test method for a small room configuration*, ISO 9705-1:2016(E), Vernier, Geneva, Switzerland, (2016). [Online]. Available: https://www.iso.org/standard/59895.html

[21] B. F. Magnussen and B. H. Hjertager, "On mathematical modeling of turbulent combustion with special emphasis on soot formation and combustion," *Symposium (International) on Combustion,* vol. 16, no. 1, pp. 719-729, (1977), doi: https://doi.org/10.1016/S0082-0784(77)80366-4.

[22] B. F. Magnussen, "On the structure of turbulence and a generalized eddy dissipation concept for chemical reactions in turbulent flow," presented at the 9th AIAA Society Meeting, St. Louis, MO, USA, 1981).

[23] A. L. Brown, B. W. Lance, N. P. Grieb, M. Clemenson, M. Benson, and C. Elkins, *Dispersion Validation for Urban Flow in Downtown Oklahoma City*, Sandia National Laboratories, SAND2020-10131, 2020).

[24] A. L. Brown *et al.*, "Proceedings of the first workshop organized by the IAFSS working group on measurement and computation of fire phenomena (MaCFP)," *Fire Safety Journal,* vol. 101, pp. 1-17, (2018). [Online]. Available: https://doi.org/10.1016/j.firesaf.2018.08.009.

[25] N. M. Marinov, C. K. Westbrook, and W. J. Pitz, "Detailed and Global Chemical Kinetics Model for Hydrogen," presented at the 8th International Symposium on Transport Properties, San Francisco, California, United States, (March 1995). Available: https://www.osti.gov/servlets/purl/90098.

[26] M. Hertzberg, "Flammability limits and pressure development in H2-air mixtures," presented at the Workshop on the Impact of Hydrogen on Water Reactor Safety, Albuquerque, NM, United States, pp. 13-67, (September, 1981), NUREG/CR--2017-Vol3. Available: http://inis.iaea.org/search/search.aspx?orig_q=RN:15046472.

[27] F. J. Benz and P. L. Boucher, "Flammability characteristics of hydrogen/oxygen/nitrogen mixtures at reduced pressures," presented at the Workshop on the Impact of Hydrogen Water Reactor Safety, Albuquerque, NM, United States, pp. 137-169, (September, 1981), NUREG/CR--2017-Vol3. Available: http://inis.iaea.org/search/search.aspx?orig_q=RN:15047089.

[28] N. M. Marinov, W. J. Pitz, C. K. Westbrook, M. J. Castaldi, and S. M. Senkan, "Modeling of Aromatic and Polycyclic Aromatic Hydrocarbon Formation in Premixed Methane and Ethane Flames," *Combustion Science and Technology,* vol. 116-117, no. 1-6, pp. 211-287, (1996), doi: https://doi.org/10.1080/00102209608935550.

[29] D. Fernández-Galisteo, A. L. Sánchez, A. Liñán, and F. A. Williams, "One-step reduced kinetics for lean hydrogen–air deflagration," *Combustion and Flame,* vol. 156, no. 5, pp. 985-996, (2009), doi: https://doi.org/10.1016/j.combustflame.2008.10.009.

[30] A. A. Konnov, "Yet another kinetic mechanism for hydrogen combustion," *Combustion and Flame,* vol. 203, pp. 14-22, (2019), doi: https://doi.org/10.1016/j.combustflame.2019.01.032.

[31] A. A. Konnov, "Remaining uncertainties in the kinetic mechanism of hydrogen combustion," *Combustion and Flame,* vol. 152, no. 4, pp. 507-528, (2008), doi: https://doi.org/10.1016/j.combustflame.2007.10.024.

[32] J. Li, Z. Zhao, A. Kazakov, and F. L. Dryer, "An updated comprehensive kinetic model of hydrogen combustion," *International Journal of Chemical Kinetics,* vol. 36, no. 10, pp. 566-575, (2004), doi: https://doi.org/10.1002/kin.20026.

[33] J. A. Miller and R. J. Kee, "Chemical nonequilibrium effects in hydrogen-air laminar jet diffusion flames," *The Journal of Physical Chemistry,* vol. 81, no. 25, pp. 2534-2542, (1977), doi: https://doi.org/10.1021/j100540a035.

[34] M. A. Mueller, T. J. Kim, R. A. Yetter, and F. L. Dryer, "Flow reactor studies and kinetic modeling of the H2/O2 reaction," *International Journal of Chemical Kinetics,* vol. 31, no. 2, pp. 113-125, (1999), doi: https://doi.org/10.1002/(SICI)1097-4601(1999)31:2<113::AID-KIN5>3.0.CO;2-0.

[35] R. C. Rogers and W. Chinitz, "Using a global hydrogen-air combustion model in turbulent reacting flow calculations," *AIAA Journal,* vol. 21, no. 4, pp. 586-592, (1983), doi: 10.2514/3.8117.

[36] B. Sekar and H. S. Mukunda, "A computational study of direct simulation of high speed mixing layers without and with chemical heat release," *Symposium (International) on Combustion,* vol. 23, no. 1, pp. 707-713, (1991), doi: https://doi.org/10.1016/S0082-0784(06)80320-6.

[37] T. Varga *et al.*, "Optimization of a hydrogen combustion mechanism using both direct and indirect measurements," *Proceedings of the Combustion Institute,* vol. 35, no. 1, pp. 589-596, (2015), doi: https://doi.org/10.1016/j.proci.2014.06.071.

[38] C. K. Westbrook and F. L. Dryer, "Simplified Reaction Mechanisms for the Oxidation of Hydrocarbon Fuels in Flames," *Combustion Science and Technology,* vol. 27, no. 1-2, pp. 31-43, (1981), doi: https://doi.org/10.1080/00102208108946970.

[39] L. Melander and W. H. Saunders, *Reaction rates of isotopic molecules*. New York: Wiley, pp. 28-29, (1980).

[40] C. G. Swain, E. C. Stivers, J. F. Reuwer, and L. J. Schaad, "Use of Hydrogen Isotope Effects to Identify the Attacking Nucleophile in the Enolization of Ketones Catalyzed by Acetic Acid1-3," *Journal of the American Chemical Society,* vol. 80, no. 21, pp. 5885-5893, (1958), doi: https://doi.org/10.1021/ja01554a077.

[41] E. S. Lewis and J. K. Robinson, "The influence of tunneling on the relation between tritium and deuterium isotope effects. The exchange of 2-nitropropane-2-t," *Journal of the American Chemical Society,* vol. 90, no. 16, pp. 4337-4344, (1968), doi: https://doi.org/10.1021/ja01018a025.

[42] M. J. Stern and R. E. Weston, "Phenomenological manifestations of quantum-mechanical tunneling. III. Effect on relative tritium-deuterium kinetic isotope effects," *The Journal of Chemical Physics,* vol. 60, no. 7, pp. 2815-2821, (1974), doi: https://doi.org/10.1063/1.1681449.

[43] L. C. Cadwallader and D. A. Petti, "Deuterium and Tritium Safety Issues in IFE Target Fabrication," *Fusion Science and Technology,* vol. 41, no. 3P2, pp. 635-641, (2002), doi: https://doi.org/10.13182/FST02-A22665.